

## FEASIBILITY ANALYSIS OF GPS III INTEGRATED WITH AN INERTIAL SYSTEM TO PROVIDE CAT IIIB SERVICES

Young C. Lee, Curtis A. Shively, MITRE/CAASD

**Dr. Young C. Lee** is a member of the Principal Staff at the Center for Advanced Aviation System Development (CAASD) of the MITRE Corporation. He has been working in the area of GPS integrity since 1986 in support of the Federal Aviation Administration (FAA). He also has been serving as secretary of RTCA SC-159 and as co-chairman of its GPS/Inertial Working Group. He received his B.S. from Seoul National University in Korea and his Ph.D. from the University of Virginia, both in electrical engineering.

**Curtis A. Shively** is a member of the Principal Staff at MITRE/CAASD. He has studied the use of satellites for communications, navigation and surveillance. He received his B.S. and M.S. in Electrical Engineering from the Massachusetts Institute of Technology.

### Abstract

This paper describes a follow-on analysis of the potential for an integrated GPS III/inertial reference system (IRS) to provide Category IIIB (CAT IIIB) precision approach and landing services. Three different levels of GPS III capability are considered: 1) one without cross-link (GPS IIIA), 2) one with cross-link but without improved integrity assurance (GPS IIIB), and 3) one with cross-link also providing improved integrity assurance (GPS IIIC). The CAT IIIB landing requirements are expressed as constraints on the vertical navigation sensor error (NSE) to ensure a high probability of safe landing under both fault-free and faulted conditions. In particular the most restrictive requirement dictates the probability of missed detection of a satellite fault resulting in erroneous range measurements. GPS fault detection is performed by applying a threshold to the innovation residual (difference between predicted and measured ranges). A Monte Carlo simulation is used to estimate the missed detection performance of the integrated system. Both step faults and ramp faults are considered. The integrated system comprises an IRS with navigation grade sensors tightly coupled with a GPS receiver using pseudorange and possibly also delta range measurements to continuously update corrections to the inertial measurements. Results indicate that an inertial system integrated with a GPS receiver using delta range measurements could likely meet the CAT IIIB fault detection requirements for any step or ramp faults during the timeframe of any of the three phases of GPS III implementations. However, if the delta range measurements are not used, the CAT IIIB requirements could only be met with GPS IIIC.

### Introduction

Many papers have previously been published on integrated GPS/inertial reference system (IRS) solutions to improve primarily continuity but also availability of service upon loss of GPS signals, which could be caused by intentional or unintentional GPS interference, occasional

periods of poor user-to-satellite geometry or by ionospheric scintillation, for example [1, 2, 3]. However, most studies concerned with GPS civil aviation applications have focused on the capability required for Required Navigation Performance (RNP) operations, including lateral guidance during nonprecision approaches. Recently with the expectation of much improved GPS performance in the future, interest has shifted to the feasibility of supporting more demanding navigation applications without having to rely on external augmentations to GPS. In particular, the GNSS Evolutionary Architecture Study (GEAS) Panel has evaluated a GPS-based architecture using advanced receiver autonomous integrity monitoring (ARAIM) to provide robust worldwide instrument approach guidance known as LPV-200 in the 2025–2030 time frame [4, 5]. With dual-frequency civil signal transmissions and enhanced ground and space segment monitoring and processing, a significant improvement in signal-in-space (SIS) accuracy is expected from the modernized GPS.

The current study is a follow-on of our earlier study [6] to evaluate the feasibility in the GPS III time frame of using a GPS receiver integrated with an IRS with navigation grade sensors in the avionics to provide robust CAT IIIB service worldwide. The CAT IIIB landing requirements are very demanding and the vertical guidance requirements are the most difficult to achieve. As in most GNSS-based systems, the major issue is not accuracy but integrity and the availability of service with integrity. While the accuracy that can be provided with GPS III alone might meet the CAT IIIB requirements with adequate availability, the integrity requirements could not be met without inertial integration, as shown in our earlier study [6].

The current study considers three different levels of GPS III capabilities consistent with the planned implementation of GPS III in three phases progressing from GPS IIIA to GPS IIIC as shown in Table 1 [7].

Table 1. Expected GPS III Capabilities

	GPS IIIA	GPS IIIB	GPS IIIC
Range Error Bound	4.42 URA (*)	4.42 URA	5.73 URA
Integrity Level	$10^{-5}/\text{SV/hr}$	$10^{-5}/\text{SV/hr}$	$10^{-8}/\text{SV/hr}$
Time-to-alert	10 sec	10 sec	5.2 sec
Cross-link	No	Yes	Yes

(\*) URA (User Range Accuracy) is a quantity broadcast by GPS satellites that characterizes the user range measurement errors associated with the control and space segments.

For GPS IIIA the nominal SIS error will likely be smaller than it is with Block II satellites now on orbit. However, since the satellite ephemeris data and on-board satellite clock correction can only be updated a few times per day by the ground system, the SIS range error will remain relatively large. GPS IIIB is planned to have a cross-link capability allowing frequent update of the data band thus providing smaller SIS error but will not provide improved integrity assurance. GPS IIIC will provide not only quick updates of the data using the cross-link capability but also improved integrity assurance. A much reduced probability of SIS faults can be assumed with the GPS IIIC satellites because GPS IIIC satellites will be equipped with built-in capabilities to detect clock failures and other on-board hardware/software faults, and the GPS III control segment will be designed to validate commands and uploads before they are transmitted to the satellites. However, even GPS IIIC SIS integrity performance is constrained by a 5.2 sec time-

to-alert, while CAT IIIB operations require a time-to-alert of 2 sec or less. Also the fault detection performance provided by GPS IIIC may not be sufficient without inertial integration to meet the CAT IIIB requirements.

Our earlier study in [6] focused on GPS IIIC because it was believed to provide the best chance to achieve CAT IIIB performance. The current study extends the earlier analysis and evaluates the feasibility of achieving CAT IIIB performance for all three phases of GPS III implementations.

The remainder of the paper has four main sections. In the next section, the CAT IIIB navigation system error (NSE) requirements are reviewed. This is followed by a description of the GPS/inertial system model, performance evaluation methodologies, and assumptions for the performance analysis. Subsequently the results of a Monte-Carlo simulation analysis of integrity performance, expressed in terms of fault detection (or equivalently missed detection) performance, are presented. The paper concludes with a summary and a discussion of future work.

### CAT IIIB NSE REQUIREMENTS

Category IIIB (CAT IIIB) operations encompass not only precision approach, but also landing and rollout. Therefore, the performance requirements for CAT IIIB are expressed in terms of probability of a safe landing as represented by the touchdown point of the aircraft on the runway. The touchdown point is related to the total system error ( $TSE$ ), which is modeled as the sum of two components: 1) flight technical error ( $FTE$ ) related to the aircraft landing system's ability to keep the aircraft on the desired path and 2) navigation sensor error ( $NSE$ ) related to the accuracy of the aircraft's actual position estimate. For a practical application, consideration must of course be given to landing performance in both the lateral and longitudinal dimensions. For the type of performance analysis in this paper, however, the longitudinal touchdown performance is often assumed to have a simple linear relationship to the vertical  $NSE$  ( $NSE_V$ ). Furthermore, it is also commonly recognized that safe landing places more stringent requirements on vertical  $NSE$  than on lateral  $NSE$ . Therefore, only the longitudinal dimension of  $TSE$  (vertical dimension of  $NSE$ ) will be considered herein.

The safe landing requirements addressed in this paper were developed for achieving CAT IIIB performance using ground-based augmentation system (GBAS). A new terminology was adopted by the GBAS community according to which this capability is referred to as GBAS Approach Service Type D (GAST D). The technical concept for GAST D is extensively described in various papers, including [8]. The GAST D concept meets NSE performance requirements formulated to address three circumstances: 1) fault-free nominal condition, 2) faulted limit case, and 3) faulted malfunction case. Thorough derivations and discussions of these requirements, particularly the two faulted cases, have been presented previously in several sources, including [8–12]. For the convenience of the reader, the derivations and assumptions used in this analysis are summarized in Appendix A of our earlier paper [6]. Only a brief description of the derivation and its results are presented immediately below.

*Nominal Condition.* Under fault-free conditions the probability of unsafe landing must not exceed  $10^{-6}$ . Given assumptions for  $FTE$  and the approach glide path angle ( $GPA$ ), this requirement restricts the standard deviation of a Normal distribution characterizing  $NSE_V$

$$\sigma_{NSE_V, \text{fault-free}} \leq 2.38 \text{ m} = 7.82 \text{ ft} \tag{1}$$

*Limit Case.* Given that a fault is present, the probability of unsafe landing must not exceed  $10^{-5}$ . This requirement places a restriction on the probability of missed detection ( $P_{md}$ ) of the vertical error bias produced by the fault,  $NSE_{V, \text{fault-bias}}$ . The resulting  $P_{md}$  restriction is shown in Figure 1. Note that the allowable  $P_{md}$  increases for decreasing vertical error bias values and may be as large as 1.0 (never detected) for  $NSE_{V, \text{fault-bias}}$  smaller than about 1.8 m.

*Malfunction Case.* For faults more likely than  $10^{-9}$ , the landing must be safe with complete certainty (probability 1.0). Since the malfunction case includes the prior probability of fault,  $P_{\text{fault}}$ , the product of  $P_{\text{fault}}$  and  $P_{md}$  must not exceed  $10^{-9}$  for any fault larger than the particular value,  $E_{V, \text{safe\_max}}$ , that would make the landing unsafe. For the assumptions in this analysis  $E_{V, \text{safe\_max}} = 7.2 \text{ m}$  (See Appendix A in [6]). Thus, an equivalent restriction inversely proportional to  $P_{\text{fault}}$  is placed on  $P_{md}$  for any value of  $NSE_{V, \text{fault-bias}}$  larger than 7.2 m. The resulting  $P_{md}$  restriction for several values of  $P_{\text{fault\_per\_hour}}$  is also shown in Figure 1. (See Appendix A in [6] for the relationship between  $P_{\text{fault}}$  and  $P_{\text{fault\_per\_hour}}$ .) Note for example that for  $P_{\text{fault\_per\_hour}} = 10^{-4}$  to  $10^{-5}$  there is a region of  $NSE_{V, \text{fault-bias}}$  where the malfunction case requirement is more restrictive than the limit case requirement. However, for  $P_{\text{fault\_per\_hour}} = 10^{-6}$ , the malfunction case requirement has no effect.

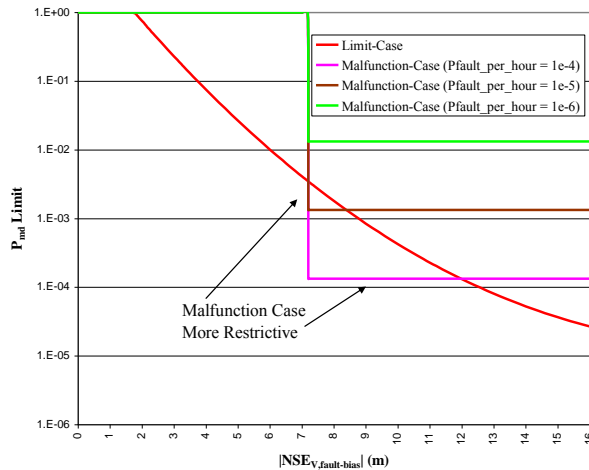


**Figure 1.  $P_{md}$  Limit versus  $NSE_{V, \text{fault-bias}}$  for Limit Case and Malfunction Case**

## SYSTEM DESCRIPTION, ASSUMPTIONS, AND EVALUATION METHODOLOGIES

### GPS/Inertial System Architecture

The system architecture used as the basis of our simulation model is a tightly coupled GPS/inertial system described in detail in [1, 13] and illustrated in Figure 2. As shown, the system consists of three units: a GPS receiver, an IRS, and an integration processor (IP). The IRS generates inertial solutions in an *open loop* mode and passes the information to the IP. The GPS receiver generates the pseudorange (PR) measurements and computes satellite positions and passes these data to the IP. Using these inputs from the GPS receiver and the IRS, the IP generates the navigation solution by correcting the IRS solutions using a Kalman filter.

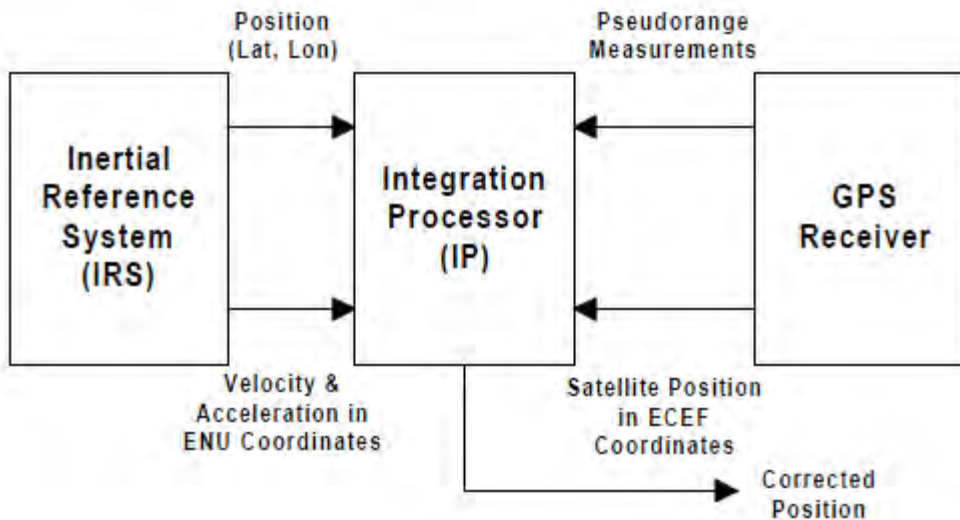


**Figure 2. System Architecture for a Tightly Coupled GPS/Inertial System**

A navigation grade inertial sensor is assumed for the IRS and a good quality temperature-controlled crystal oscillator clock is assumed for the GPS receiver [3]. The satellite range measurements used by the Kalman filter are of two types: PRs and delta PRs. The delta PR is the rate of change of PR taken from the carrier tracking loop. The measurements received at a 1 Hz rate are averaged over every Kalman filter update cycle of 10 sec. With the high frequency error components removed in this manner, the remaining components of the measurement errors are modeled as satellite bias errors with correlation time constants of 1 hr. A total of 24 error states defined for the Kalman filter include 16 IRS error states, 2 user clock error states and 6 satellite range bias error states. Since the vertical channel of an inertial system is typically quite stable over short periods of time, it is expected that there will be no significant inertial error growth during a short delay time. For this reason, the vertical position error is directly estimated in the Kalman filter rather than from the baro-inertial altimeter integration that has traditionally been used.

### Assumptions for Simulation

The Monte-Carlo simulation is performed under the following assumptions.

- The IRS has triple redundancy and thus is assumed never to fail. The IRS has navigation grade inertial sensors.
- A 60-min flight is assumed which includes two 180-deg turns, one at the beginning of the flight and the other at the end, immediately before a presumed approach and landing. It is assumed that calibration of the inertial system starts at the beginning of the flight, but the integrity performance is evaluated only during the last 2.5 min of the flight, i.e., the precision approach.
- A single location in the conterminous United States is assumed.
- The nominal 24-satellite GPS constellation is assumed. For the sake of simplicity, only a fixed number (6) of satellites that are visible to the user during the entire flight are used as ranging sources.
- Two cases are considered regarding the type of range measurements. In the first case, only PRs are used. In the second case, both PRs and delta PRs are used together. In general, the use of delta PRs can greatly improve performance, but it also leads to a more complex implementation. For example, it requires a precise lever arm correction, and attention needs to be paid to the effects of possible cycle slips.
- Two parameters are defined regarding the range measurement errors: 1) the standard deviation of high frequency satellite range error averaged over the Kalman Filter update cycle ( $\sqrt{R_k}$ ) characterizing the measurement noise and 2) the standard deviation of the range bias error assumed to have 1-hour correlation time constant ( $\sqrt{Q_k}$ ) representing the process noise for the range bias error states. In this analysis, ( $\sqrt{R_k}$ ) and  $\sqrt{Q_k}$  values are derived from the values of 0.25 m and 0.1 m previously assumed by GEAS [4, 5] for User Range Error (URE) and nominal bias magnitude, respectively, along with the GEAS user range error model. However, these values assumed by GEAS apply to zero age of data, i.e., they assume frequent updates of the navigation data via cross-links. Since the cross-link will not be implemented until GPS IIIB, the GEAS values are assumed for GPS IIIB and GPS IIIC while these values are doubled for GPS IIIA. The standard deviation of delta PR is assumed to be 0.5 cm/sec.
- Since CAT IIIB requirements are more stringent for vertical *NSE* than for lateral *NSE*, the focus is placed on the vertical position error performance in our analysis.

### Fault-Free Performance

Our earlier study [6] provided the simulation results of the vertical position error in the absence of a fault over the flight duration of 60 min (without using delta PR). It was then observed that one standard deviation of the vertical position error in steady state remains well below the fault-free vertical error requirement of 2.38 m in Eq. (1). While this observation applies to a specific set of assumptions regarding user-to-satellite geometry, it suggests that it might possible to meet this fault-free vertical error requirement in general.

## Methodologies for Faulted Performance Evaluation

In this study, integrity performance is evaluated via a Monte Carlo analysis to determine the probability of missed detection ( $P_{md}$ ) in the presence of a fault. It is assumed that a fault may cause one of two types of errors: ramp error or step error. Since a fault can occur at any time, errors of each of these types are introduced at various times and with different magnitudes. The resulting test statistics and the vertical position errors are then calculated and the missed detection events counted.

### Introduction of a fault

It is assumed that the ramp error starts exactly at a Kalman filter update time and the step error starts midway between two successive update times. Different times have also been investigated but the results are not significantly different.

### Measurement vector

When there are  $N$  satellites and only PR measurements are used, the length of the measurement vector is  $N$ . When delta PRs are also used, the measurement vector has  $N$  additional elements for the delta PRs.

### Fault detection scheme

For fault detection, a scheme that was originally proposed by Dr. John Diesel of Litton for his AIME algorithm is used in this paper. The scheme, which is described in detail in [14], uses the normalized innovation residual, which was shown to have a chi-square distribution, central in the absence of a fault and non-central in the presence of a fault. Following the methodology proposed for AIME, this paper calculates multiple test statistics at each Kalman filter update time with each test static obtained by averaging the normalized innovation residuals over the past  $N$  Kalman filter update cycles for up to 5 min. This is done to maximize the detection capability of a fault causing a slowly increasing error. If any of the multiple test statistics exceeds the detection threshold, a fault detection is declared. The detection threshold is determined conservatively by assuming that the multiple test statistics are all independent.

### $P_{md}$ evaluation methodology

While test statistics are calculated at each Kalman filter update time ( $t_k$ ), the position error that results from ramp or step errors combined with random range errors is calculated every receiver processing time interval (assumed to be every second). The position error between Kalman filter update times is extrapolated from the last position update and the last vertical velocity estimate. Then depending on the fault detection result and the size of the position error relative to the position error bound ( $E_v$ ), one of four possible outcomes is declared: missed detection, early detection, timely detection, or no event. In the determination of the outcome, the 2-sec time-to-alert allowed for CAT IIIB operations is taken into consideration. This process was described in detail in our earlier paper [6].

### Duration of $P_{md}$ Evaluation

It is assumed that a fault of any size may start (in the case of a ramp) or occur (in the case of a step) any time before or during the Precision Approach (PA), missed detection events are counted only during the PA. An assumption is made that the detection mechanism in place for CAT IIIB would always detect a fault that occurs prior to the PA before the position error exceeds the relatively large alert limit that applies before the precision approach. Also if a detection flag is raised before the PA starts, it is counted as an early detection.

### **PROBABILITY OF MISSED DETECTION PERFORMANCE RESULTS**

In general,  $P_{md}$  depends on the following factors.

- Fault type (ramp or step)
- Measurements processed by the user receiver (PRs only or both PRs and Delta PRs)
- Timing of the fault, that is, time offset of the fault occurrence time with respect to the PA start time
- Fault size
- Ev bound
- GPS capability in terms of accuracy and integrity (GPS IIIA, IIIB, or IIIC)

$P_{md}$  has been obtained via simulation for different combinations of these factors as discussed below. The first few plots show  $P_{md}$  in the presence of a ramp fault as a function of ramp start time and ramp rate for different GPS III capabilities when only PRs are used. The second set of plots show the maximum  $P_{md}$  obtained as a function of Ev bound against the CAT IIIB requirements for different GPS III capabilities.

### **$P_{md}$ in the Presence of Ramp Fault as a Function of Ramp Start Time and Ramp Rate**

Figure 3 shows  $P_{md}$  when only pseudorange measurements are used with GPS IIIA for an Ev bounds of 4 m, as an example. The figure shows that  $P_{md}$  varies widely as a function of ramp slope and ramp start time offset. A ramp fault can start at any time and cause an integrity failure during the PA, but the figure shows that the maximum  $P_{md}$  occurs when the ramp starts sometime between 1 minute before, and 1 minute after, the start time of the PA. Also, for any given ramp start time offset, the  $P_{md}$  is the highest somewhere between ramp rates of 0.01 and 0.1 m/s. This observation can be explained as follows.



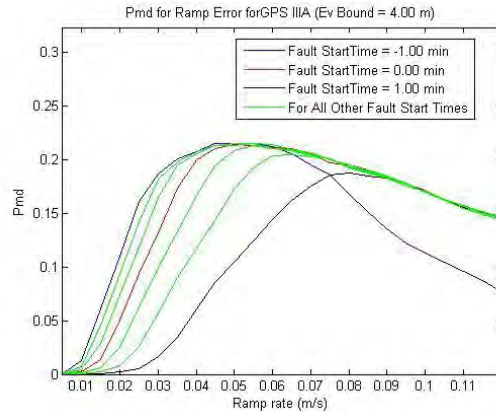


**Figure 3.**  
 **$P_{md}$  for a Ramp Fault for GPS IIIA**  
**(Without Delta Range, Ev bound = 4 m)**

Figure 4 shows the percentage of detection flags raised for the first time at each Kalman filter update cycle for the case of ramp start time offset of  $(-1)$  min, as an example. It is assumed that a condition in which the position error exceeds the Ev bound is of no significance if it occurs prior to the PA start. For this reason, as long as a detection flag is raised prior to the PA start by the airborne processing, the event is counted as an early detection regardless of whether the position error has exceeded Ev bound or not. Therefore, the higher the ramp rate (e.g., much larger than 0.06 m/s shown in this example), the higher the probability of a detection flag being raised early, causing an early detection and thus lowering  $P_{md}$ . On the other hand, if the ramp rate is low (e.g., much less than 0.03 m/s shown in this example), the probability that the position error would exceed the Ev bound would remain low throughout the PA, thus resulting in a low  $P_{md}$ . Therefore,  $P_{md}$  peaks at a ramp rate between the two extremes.

As stated earlier, missed detection events are counted only when they occur during the PA. All detections that occur prior to the PA are counted as early detections. It is also noted that with GPS IIIC, credit is given to integrity alerts from GPS IIIC when counting missed detection events. That is, if a fault occurs, any missed detection event that occurs more than 5.2 seconds after the range error due to the faults exceeds 5.73 times URA is not counted as a missed detection, even if it occurs during the PA. Of course, if an event occurs in which the position error exceeds its Ev bound without a detection flag before the range error caused by the fault reaches 5.73 times the URA during the PA, it will be counted as a missed detection.

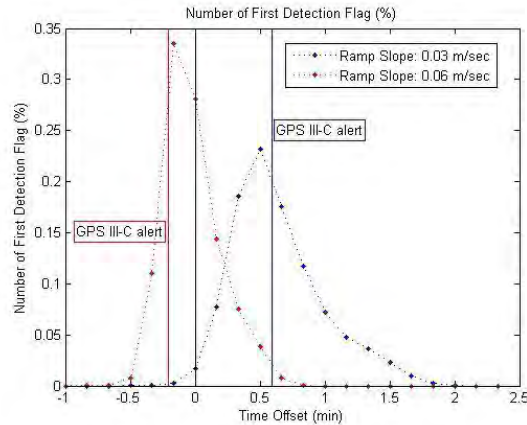


**Figure 4.**  
**Percentage of First Detection Flags as Functions of Time Offset**  
**(Ramp Start Time Offset = -1 min)**

$P_{md}$  for GPS IIIB is shown in Figure 5. In this case,  $P_{md}$  is smaller than for GPS IIIA because, with the cross-link capability, GPS IIIB can provide more accurate range measurements. Thus, the IRS can be calibrated more precisely and provides better capability to detect subsequent GPS SIS faults. Again the peak  $P_{md}$  occurs when the ramp starts sometime between 1 minute before, and 1 minute after, the start time of the PA, and the ramp rate is between 0.01 and 0.1 m/s.

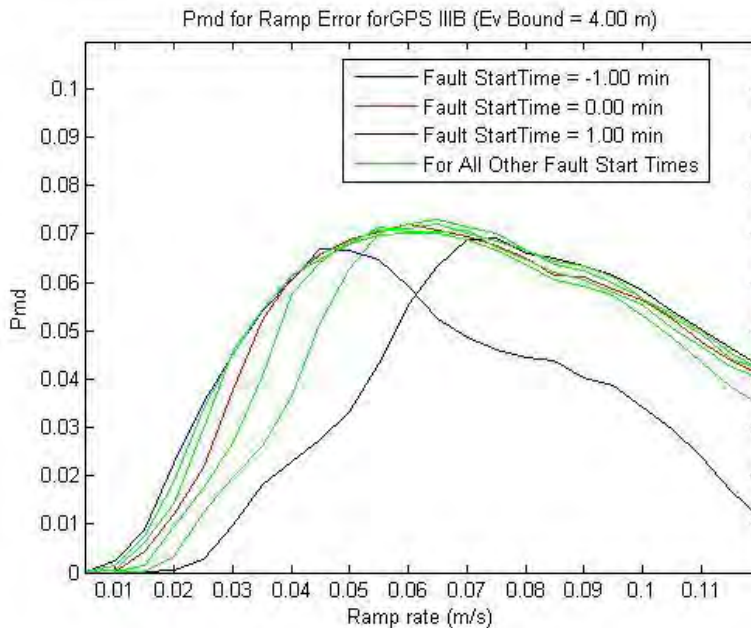


**Figure 5.**  
**Observed  $P_{md}$  for a Ramp Fault for GPS IIIB**  
**(Without Delta Range, Ev bound = 4 m)**

$P_{md}$  for GPS IIIC shown in Figure 6 is even smaller since credit is given to GPS IIIC integrity alerts. As stated earlier, credit is given to the integrity alert capability for GPS IIIC when counting missed detections. The time at which the range error reaches 5.73 times URA varies with the error start time and the ramp rate. For a higher ramp rate, the range error reaches 5.73

times URA earlier but an initial missed detection is more likely. For a lower ramp rate, a missed detection may occur more slowly, but the time period in which a missed detection may occur is longer. This explains why  $P_{md}$  fluctuates for ramp rates above 0.04 m/s in Figure 6.

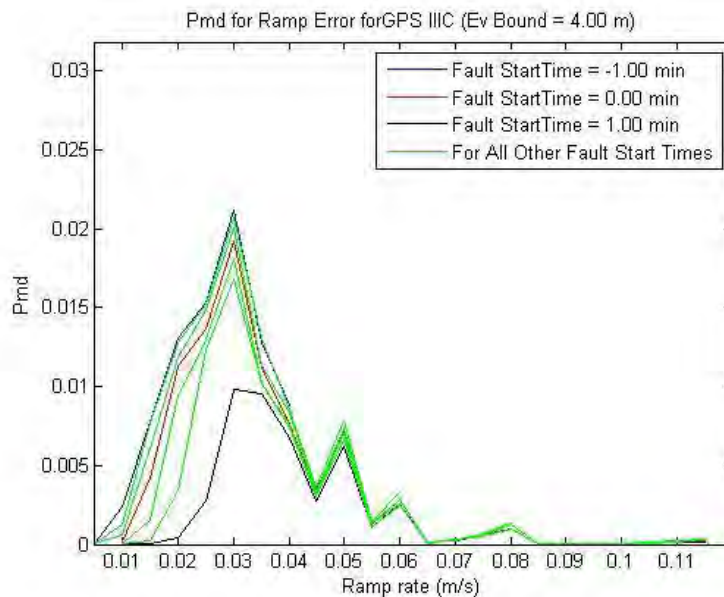


**Figure 6.**  
**Observed  $P_{md}$  for a Ramp Fault for GPS IIC**  
**(Without Delta Range, Ev bound = 4 m)**

### Maximum $P_{md}$ with and without Delta Range Measurements in the Presence of a Ramp Fault

$P_{md}$  varies widely depending on the fault start time and ramp rate. However,  $P_{md}$  cannot exceed the maximum  $P_{md}$  value for each given Ev bound regardless of the condition. These maximum  $P_{md}$  values are taken for all Ev bounds of interest and compared against the CAT IIIB requirements discussed earlier. They are plotted in Figures 7 to 9, each comparing  $P_{md}$  between two cases, one without and the other with delta range measurements. Figures 10 to 12 show the same types of results for step faults.

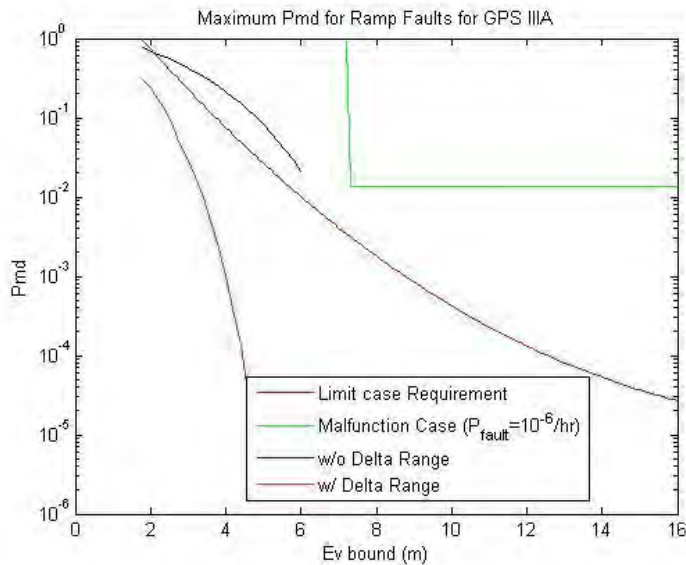
Note that the requirement for the malfunction case varies with the prior probability of fault per hour. Table 2 shows the assumptions for ramp and step fault error size with associated probabilities [15]. For ramp fault error rates (0.01 m/s to 0.75 m/s) causing relatively large  $P_{md}$  values, the probability of occurrence is  $10^{-6}/SV/hr$ . For the step fault error, the probability of occurrence is  $10^{-4}/SV/hr$ .

**Table 2 Assumptions for Integrity Assured GPS III [15]**

Fault type	Fault error rate	Error probability
Ramp	0.01 m/s to 0.05 m/s	$10^{-6}/\text{SV/hr}$
	0.05 m/s to 0.25 m/s	$10^{-6}/\text{SV/hr}$
	0.25 m/s to 0.75 m/s	$10^{-6}/\text{SV/hr}$
	0.75 m/s to 2.5 m/s	$3.5 \times 10^{-6}/\text{SV/hr}$
	2.5 m/s to 5 m/s	$4.1 \times 10^{-6}/\text{SV/hr}$
	0.01 m/s and larger	$10^{-4}/\text{SV/hr}$
Step		$10^{-4}/\text{SV/hr}$

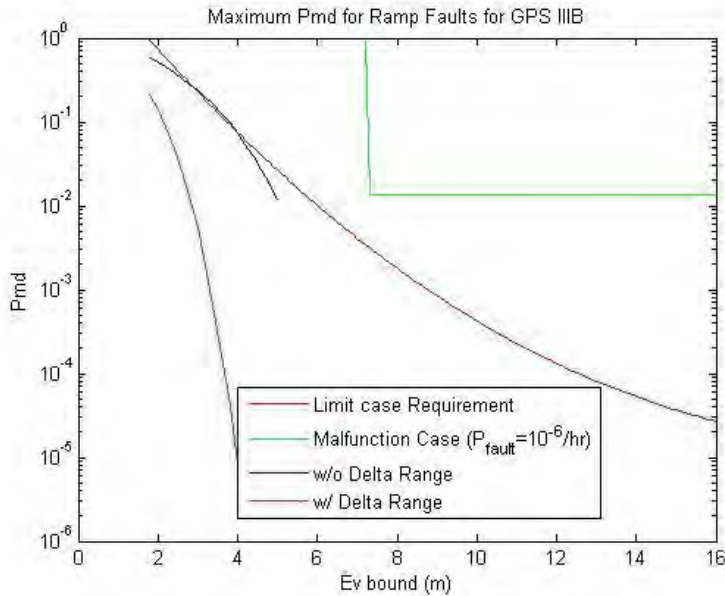
A value of  $10^{-4}$  applies for step faults and a value of  $10^{-6}$  applies for ramp faults [15].

Figure 7 shows maximum  $P_{md}$  results for GPS IIIA in the presence of a ramp fault. These results indicate that during the GPS IIIA time period, the CAT IIIB requirements can be met for ramp type faults if delta range measurements are used.



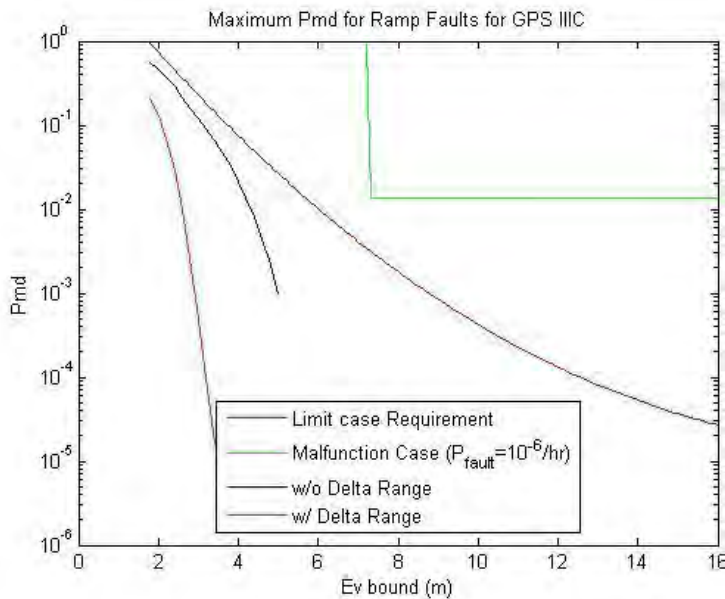
**Figure 7. Maximum  $P_{md}$  for Ramp Faults for GPS IIIA versus  $P_{md}$  Requirements**

Figure 8 shows maximum  $P_{md}$  results for GPS IIIB in the presence of a ramp fault. It is observed that in the case with no delta range measurements,  $P_{md}$  coincides with the limit case CAT IIIB requirement for Ev bounds between approximately 2 m and 4 m with no margin. This result is a little different from that obtained in the earlier analysis [6]. The difference comes from a small change in the assumptions regarding the ramp start time. In the earlier analysis, both the duration of the simulation for  $P_{md}$  determination and the duration of a ramp fault were limited to 1 min. In the present analysis, the duration of the simulation includes the full 2.5 min duration of PA and a ramp fault is allowed to start any time before or after the PA start time. In case delta range measurements are used, the CAT IIIB requirements could be met with more margin with GPS IIIB than with GPS IIIA.



**Figure 8. Maximum  $P_{md}$  for Ramp Faults for GPS IIIB versus  $P_{md}$  Requirements**

Figure 9 shows maximum  $P_{md}$  results for GPS IIIC in the presence of a ramp fault. It is observed that CAT IIIB requirements can be met without using delta range measurements.



**Figure 9. Maximum  $P_{md}$  for Ramp Faults for GPS IIIC versus  $P_{md}$  Requirements**

**Maximum  $P_{md}$  with and without Delta Range Measurements in the Presence of a Step Fault**

Figure 10 shows the maximum  $P_{md}$  for GPS IIIA in the presence of a step fault. Like the case of a ramp fault shown in Figure 7, the CAT IIIB requirements cannot be met without using delta range measurements. However, dramatically smaller  $P_{md}$  are obtained with delta range

measurements. This is expected because velocity is obtained with delta range measurements and a step fault causes a sudden jump in velocity. Figures 11 and 12 show that the CAT IIIB requirements can be met in either the GPS IIIB or IIIC time frame even when delta range measurements are not used. When the delta range measurements are used,  $P_{md}$  is negligibly small for these cases.

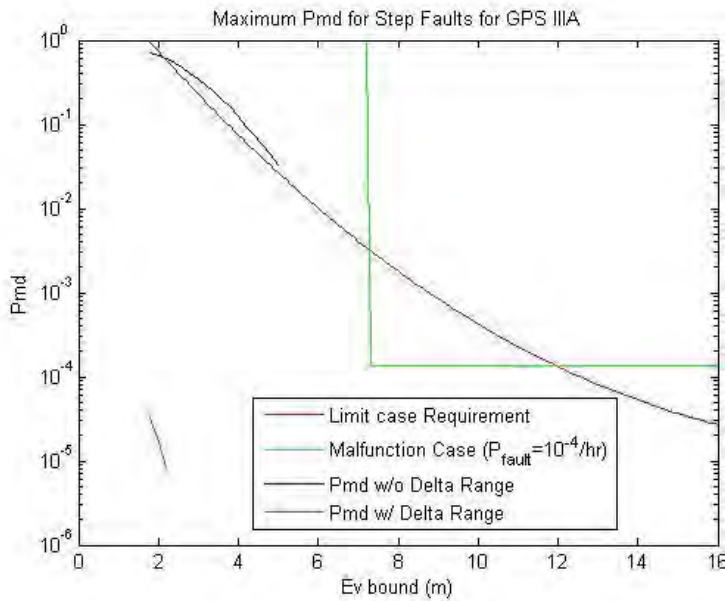


Figure 10. Maximum  $P_{md}$  for Step Faults for GPS IIIA versus  $P_{md}$  Requirements

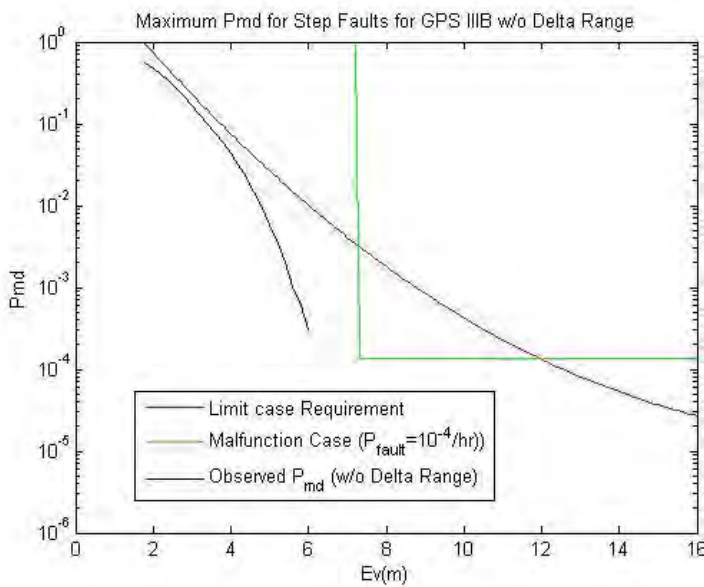
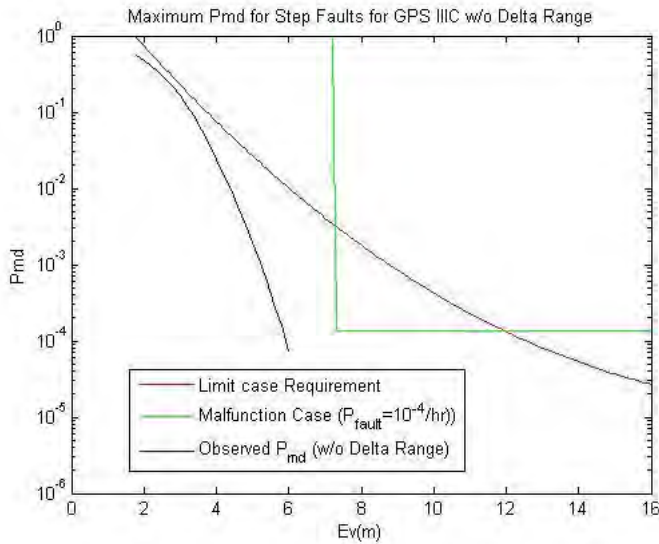


Figure 11. Maximum  $P_{md}$  for Step Faults for GPS IIIB versus  $P_{md}$  Requirements



**Figure 12. Maximum  $P_{md}$  for Step Faults for GPS IIIC versus  $P_{md}$  Requirements**

In the above discussion, the maximum  $P_{md}$  for ramp and step faults have been separately evaluated against the CAT IIIB  $P_{md}$  requirements. Since the requirements must be met regardless of the fault type, the above evaluations can be summarized as follows.

- If the delta range measurements are used, CAT IIIB requirements can be met starting from the GPS IIIA time period.
- If the delta range measurements cannot be used, CAT IIIB requirements can be met only during the GPS IIIC time period. It should be noted that for the GPS IIIB time period, the  $P_{md}$  performance based on the specific assumptions in this analysis would just barely exceed the allowed limit.

### Summary

The study is a follow-on evaluation of the performance of a GPS receiver integrated with an IRS with navigation grade sensors in the GPS III timeframe (GPS IIIA, IIIB and IIIC) to determine if CAT IIIB requirements can be met. The evaluation was done using a Monte-Carlo simulation:

- It was assumed that a fault would cause either a ramp error or a step error. These types of errors with varying magnitudes were introduced in the measurements. A missed detection was defined to be an event in which the vertical position error ( $E_v$ ) exceeds a specified  $E_v$  bound and yet no detection flag is raised within 2 sec of the event. It was shown that for any given  $E_v$  bound, the probability of missed detection ( $P_{md}$ ) evaluated via Monte Carlo simulation varies widely as a function of several factors including the fault start time and the

error magnitude caused by the fault. Out of the values obtained, the largest  $P_{md}$  was taken for each Ev bound. The largest  $P_{md}$  values were compared to the CAT IIIB requirements.

- The results obtained showed that, even without using delta PR measurements, a GPS receiver integrated with a navigation grade inertial system could likely meet the CAT IIIB integrity performance requirements in the GPS IIIC timeframe. If delta PR measurements can be used, the CAT IIIB requirements can also be met starting in the GPS IIIA period. As noted earlier, use of delta PRs requires a more complex implementation. For example, such issues as a precise lever arm correction and cycle slips need to be addressed.
- The results were obtained for a single location using a flight profile involving two 180 deg turns, one at the beginning of the flight and the other toward the end, and using six satellites that are visible to the user throughout the entire flight. While this flight profile does not involve a great variety of conditions, it is believed to be adequate to ensure representative results. For this reason, it was surmised that, in the GPS IIIC timeframe, a GPS receiver integrated with a navigation grade inertial system could meet the CAT IIIB integrity performance with acceptable availability

### **Future work**

The current study of a GPS receiver integrated with an inertial system to provide the CAT IIIB services in the GPS III timeframe has yielded some promising results regarding its feasibility. However, the study will be expanded to address a number of issues, in particular:

- For the assumptions in the present study, the  $P_{md}$  performance without delta range in the GPS IIIB time period would be barely worse than allowed for ramp faults but provided some margin for step faults. Therefore, more work will be done to see if the analysis includes any conservative assumptions that, if relaxed, would make the  $P_{md}$  performance without delta range acceptable in the GPS IIIB time period.
- The present study analyzed the integrity performance via Monte Carlo simulation. In our earlier analysis [6], an attempt was made to also characterize the performance by a protection level formula derived by extending the formula for AIME HPL. However, that formula was too conservative. Further attempts to develop a formula that provides a tighter protection level have thus far been unsuccessful but will be continued in future work.
- The study has focused on integrity, that is, on the ability to detect a fault before it affects the integrity of the vertical position. That may be adequate for CAT IIIB operations. However, long before a CAT IIIB operation is initiated, it would be necessary to not only detect but also isolate a fault in order to ensure continued navigation. Such a capability would be particularly useful as a backup to GPS III (for airframes equipped with inertial systems), and would therefore partially address one of the FAA's primary concerns. For this reason, this study will also be extended to evaluate the coasting capability possible with GPS III for various service levels. The ultimate goal of this analysis is to support a future NextGen decision on PNT infrastructure and backup.



## DISCLAIMER

The contents of this material reflect the views of the authors. Neither the Federal Aviation Administration nor the Department of Transportation makes any warranty, guarantee or promise, expressed or implied, concerning the content or accuracy of the views expressed herein.

© 2009 The MITRE Corporation

## REFERENCES

1. Diesel, J. and J. King, "Integration of Navigation Systems for Fault Detection, Exclusion, and Integrity Determination—Without WAAS," *Proceedings of the National Technical Meeting of the Institute of Navigation*, Anaheim, California, 18 – 20 January 1995.
2. Brenner, M., "Integrated GPS/Inertial Fault Detection Availability," *Proceedings of The Institute of Navigation's 8th International Technical Meeting*, Palm Springs, California, September 1995.
3. Lee, Y., and S. Ericson, "Analysis of Coast Times Upon Loss of GPS Signals for Integrated GPS/Inertial Systems," *Proceedings of the Institute of Navigation National Technical Meeting 2003*, Anaheim, California, 22 – 24 January 2003.
4. *GNSS Evolutionary Architecture Study (GEAS) Phase I Report*, GEAS Panel, 24 January 2008.
5. Walter, T., et al., "Future Architectures to Provide Aviation Integrity," *Proceedings of The Institute of Navigation 2008 National Technical Meeting (NTM 2008)*, San Diego, California, 28 – 30 January 2008.
6. Lee, Y., and C. Shively, "Preliminary Feasibility Analysis of GPS IIIC Integrated with an Inertial System to Provide CAT IIIB Services," *Proceedings of 22nd International Meeting of the Satellite Division of The Institute of Navigation*, Savannah, GA, 22 – 25 September 2009.
7. Kovach, K., et al., "GPS III Integrity Concept," *Proceedings of ION GNSS 2008*, Savannah, Georgia, 16 – 19 September 2008.
8. DeCleene B., et al., "Conceptual Framework for the Proposal for GBAS to Support CAT III Operations," ICAO NSP/CSG/WP3, Toulouse, France, 8 – 10 July 2008.
9. Murphy, T., "Development of Signal in Space Requirements for GBAS to Support CAT II/III Landing Operations," *Proceedings of ION GPS 2002*, Portland, Oregon, 24 – 27 September 2002.
10. Murphy, T., "Lower Level Monitor Requirements for GSL D," ICAO NSP/WG1&2/WP64, Brussels, Belgium, 8 – 19 May 2006.

11. Shively, C., —Comparison of Methods for Deriving Ground Monitor Requirements for CAT IIIB LAAS,” *Proceedings of ION National Technical Meeting*, San Diego, California, 22 – 29 January 2007.
12. Murphy, T., —Evolution of GBAS to Support CAT II/III Operations,” briefing to GNSS Evolutionary Architecture Study (GEAS) group, 29 January 2008.
13. Lee, Y. and D. O’Laughlin, —Performance Analysis of a Tightly Coupled GPS/Inertial System for Two Integrity Monitoring Methods,” *NAVIGATION: Journal of the Institute of Navigation*, Vol. 47, No. 3, Fall 2000.
14. Diesel, J. and S. Luu, —GPS/IRS AIME: Calculation of Thresholds and Protection Radius Using Chi-Square Methods,” *Proceedings of The Institute of Navigation’s 8th International Technical Meeting*, Palm Springs, California, 12 – 15 September 1995.
15. Memorandum from Daniel P. Salvano, Director, Navigation Services, FAA to IFOR Secretariat, 26 July 2004.
16. Clark, B. and B. DeCleene, —Alert Limits: Do We Need Them for CAT III?” *Proceedings of ION GNSS 2006*, Fort Worth, Texas, 26 – 29 September 2006.